JURNAL KARTIKA KIMIA

J. Kartika Kimia, Mei 2026, 9, (1), 29-34
Journal homepage: http://jkk.unjani.ac.id/index.php/jkk
P-ISSN: 2655-1322 E-ISSN: 2655-0938

Production of CaO from Golden Snail Shells: Structural and Surface Area Characterization by XRD, FTIR, and BET Analysis

Jeanne Dewi Damayanti[1,*], Maria Assumpta Nogo Ole[2], M. Ilham Nurdin[2], Arifah Sukasri[2], Nur Amin Riyadi[2]

[1] Department of Chemical Engineering, Politeknik Negeri Ujung Pandang, Makassar, South Sulawesi, 90245, Indonesia

[2] Department of Chemical Engineering, Politeknik Negeri Ujung Pandang, Makassar, South Sulawesi, 90245, Indonesia

*E-mail: jeannedewidamayanti@poliupg.ac.id

DOI: https://doi.org/10.26874/jkk.v9i1.1077

Received: 20 Nov 2025, *Revised*: 15 May 2026, *Accepted*: 17 May 2026, *Online*: 31 May 2026

Abstract

Golden snails are widely recognized as significant pests in Indonesian rice fields because they damage young rice plants by attacking their stems and leaves. Despite their harmful agricultural impact, golden snail shells contain a high calcium carbonate ($CaCO_3$) content of approximately 60.56%, making them a valuable raw material for calcium oxide (CaO) production through calcination. In this study, golden snail shells were calcined at 700, 800, and 900°C for 5 hours. The resulting CaO materials were characterized using Fourier Transform Infrared Spectroscopy (FTIR), X-Ray Diffraction (XRD), and Brunauer Emmett Teller (BET) surface area analysis. The findings demonstrate that calcination temperature significantly influences the physicochemical properties of the produced CaO, particularly its surface area. Among the tested conditions, the sample calcined at 900°C exhibited the highest specific surface area of 244.5211 m^2/g, indicating enhanced porosity and a greater number of potential active sites at elevated calcination temperatures.

Keywords: Calcium oxide; calcination; characterization; golden snail shell

1 Introduction

One of the considered agricultural potentials in Indonesia is golden snail (*Pomacea canaliculata*), a pest of rice fields. The golden snail, which is included in the Mollusca group, reproduces very quickly, taking only 1-2 weeks to hatch. A female golden snail can produce up to 15 egg clusters over a period of 60 to 80 days, which is one full life cycle. Each cluster contains about 300 to 500 eggs [1]. The entire body of the golden snail is covered by a shell. The golden snail is a freshwater animal that has a golden shell, which is mostly consist of calcium carbonate ($CaCO_3$). Golden snail shells are composed of 60.56% $CaCO_3$, 6.72% SiO_2 and 11.82% $Ca_3(PO_4)_2$ [2].

Calcium carbonate can be converted into calcium oxide (CaO) by releasing CO_2 through heating at high temperatures which is called the calcination process. The thermal decomposition takes place through the reaction (Eq. 1).

$$CaCO_3\ (s) \rightarrow CaO\ (s) + CO_2\ (g) \qquad \text{(Equation 1)}$$

Texture, microstructure of $CaCO_3$, and its inherent chemical reactivity are several factors that influence the formation of CaO during the thermal decomposition process [3].

Calcium rich biogenic wastes, such as eggshells and oyster shells, have been widely recognized as sustainable natural sources of calcium carbonate that can be converted into high purity CaO for applications in catalysis, material development, and environmental remediation [4–7]. Like these biogenic materials, golden snail shells also contain significant calcium carbonate content, making them a promising alternative raw material for sustainable CaO production while simultaneously addressing agricultural waste management. As much as 61.95% calcium oxide was successfully obtained from golden snail shells after calcination at a temperature of 800°C [8]. The sustainable natural calcium oxide is very important to be applied in various aspects. The several roles of CaO nowadays include: adsorbents [1,9–11], catalyst [12–16], a component in glass production, an industrial

refractory material for metal smelting, an agent for paper bleaching, a neutralizer of sulfur in sugar processing, and a mediator in cosmetics and drug delivery[17], an absorbent for CO_2 capture [18–20] and inorganic-anti-microorganism materials [18].

Various biogenic calcium carbonate sources such as eggshells, oyster shells, cockle shells, and snail shells have been widely utilized for CaO production through calcination. However, studies focusing on golden snail shells from Tana Toraja are still limited. Golden snail shell waste is abundantly generated in agricultural areas and has not been optimally utilized, causing potential environmental problems. Therefore, converting this local biogenic waste into CaO provides an alternative approach for waste valorization and sustainable material development. Furthermore, the structural properties and surface characteristics of the obtained CaO may support its potential application as an adsorbent or catalyst material. This study was intended to utilize golden snail waste through a calcination process to obtain CaO. The structure of the obtained CaO was studied through characterization using FTIR, BET, and XRD.

2 Method

Golden snail shell waste was collected from rice fields in Tana Toraja, South Sulawesi, Indonesia. The shells were manually separated from the snail meat and thoroughly washed with clean water to remove adhering dirt and impurities. The cleaned shells were then sun-dried for 2 days, followed by oven drying at 150°C for 2 hours using an Ecocell oven to ensure complete removal of moisture.

Based on our previous XRF analysis, golden snail shells were confirmed to be primarily composed of $CaCO_3$ with minor impurities, including SiO_2 and phosphate compounds, establishing their suitability as a precursor for CaO production [18].

After drying, the shells were ground into powder using a pulverizer crusher operated for 5 minutes prior to thermal treatment. Calcination of the shell powder was performed using an electric muffle furnace (JFM38, Jisico, Korea) at temperatures of 700°C, 800°C, and 900°C for 5 hours. The process was conducted under atmospheric pressure (1 atm) with a heating rate of 14°C/min. After calcination, the samples were allowed to cool naturally inside the furnace to room temperature and subsequently stored in a desiccator to prevent moisture absorption.

The obtained CaO samples were characterized to determine their physicochemical properties. Fourier Transform Infrared Spectroscopy (FTIR) analysis was performed using the potassium bromide (KBr) pellet method to identify functional groups present in the samples. The spectra were recorded in the range of 4000-400 cm^{-1}. X-Ray Diffraction (XRD) analysis was conducted using Cu-Kα radiation over a 2θ range of 10-80° to determine crystalline structure and phase composition. The specific surface area was measured using the Brunauer Emmett Teller (BET) method based on nitrogen (N_2) adsorption desorption analysis.

.

3 Result and Discussion

The functional groups of the calcined calcium oxide samples were analyzed using Fourier Transform Infrared (FTIR) spectroscopy. The FTIR spectra of the purchased and calcined calcium oxide samples are shown in **Fig. 1**. The absorption bands observed at 1420 cm^{-1} and 875 cm^{-1} are attributed to the vibrational modes of carbonate (CO_3^{2-}) groups, corresponding to asymmetric stretching and out-of-plane bending vibrations, respectively. These bands indicate the possible presence of residual $CaCO_3$ or surface carbonation of CaO due to exposure to atmospheric CO_2 after calcination.

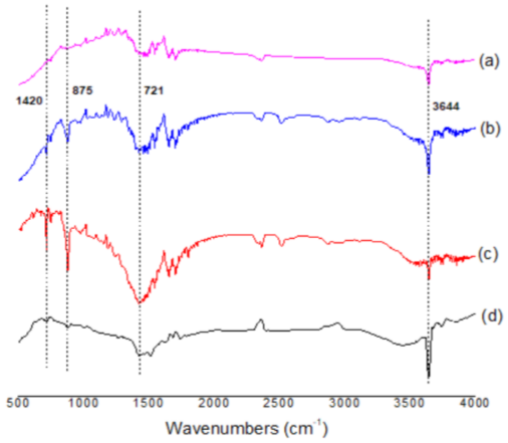

Figure 1. FT-IR spectra of (a) calcium oxide calcinated at 900°C, (b) 800°C, (c) 700°C, and (d) purchased calcium oxide.

The band observed at around 721 cm^{-1} is cautiously assigned to Ca-O lattice vibrations [19]; however, this assignment is made carefully since Ca-O vibrations are typically reported at lower wavenumbers (generally below 700 cm^{-1}), and therefore should be interpreted with reference to relevant literature.

The broad peak at approximately 3644 cm^{-1} corresponds to O-H stretching vibrations, indicating the presence of adsorbed water and/or the formation of $Ca(OH)_2$ due to hydration of CaO upon exposure to atmospheric moisture. This confirms the high hygroscopic nature of CaO, which readily reacts with water vapor in air.

Overall, the FTIR results suggest that the calcined product is predominantly CaO, which may partially convert into $Ca(OH)_2$ and $CaCO_3$ upon exposure to air after calcination [19,12].

BET analysis is performed on the calcined CaO material to measure the specific surface area of the material, which is an important indicator of various physical and chemical properties of the material. This process measures the amount of gas adsorbed on the surface of the material and, based on this data, calculates the surface area available for interaction with gas or liquid. **Fig. 2** shows that the adsorption volume of calcined CaO material increases with increasing calcination temperature, namely from 700, 800 and 900°C. The adsorption volume at 900°C is greater than the adsorption volume of purchased CaO material. The calcination process of $CaCO_3$ into CaO at high temperatures can change the size and number of pores of the CaO material. Particles can experience enlargement or the formation of new pore structures that did not previously exist. These pores can provide more space for gas molecules to occupy and be adsorbed on the surface of the material, which causes an increase in the volume of adsorbed gas.

The surface area as shown in **Table 1** was calculated with the Brunauer, Emmett and Teller (BET) Eq. 2.

$$\frac{1}{W\left(\left(\frac{P_0}{P}\right)-1\right)} = \frac{1}{W_m C} + \frac{C-1}{W_m C}\left(\frac{P}{P_0}\right) \quad \text{(Equation 2)}$$

Which W is weight of gas adsorbed; P/P^0 is relative pressure; W_m is weight of adsorbate as monolayer; and C is BET constant.

BET analysis revealed that increasing the calcination temperature led to an increase in the specific surface area of the produced CaO. The sample calcined at 900°C exhibited the highest surface area of 244.5211 m^2/g, followed by the samples calcined at 800°C and 700°C with surface areas of 232.7527 m^2/g and 205.3055 m^2/g, respectively. These values are significantly higher than that of commercial CaO (122.9513 m^2/g). The higher surface area indicates the presence of more accessible active sites, which may enhance the material's performance in adsorption, energy storage and catalytic applications.

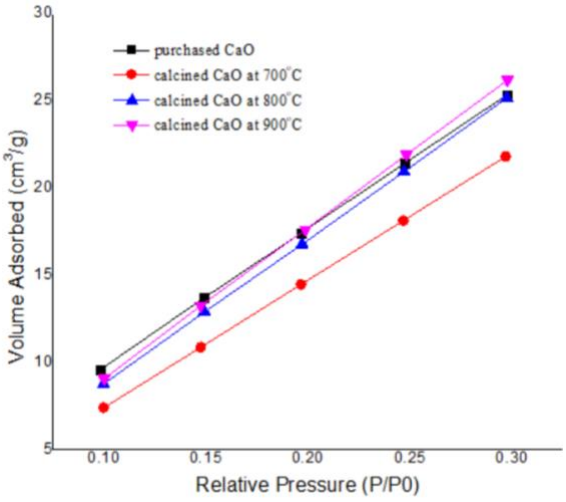

Figure 2 BET analysis result curve of gas adsorbed by calcium oxide calcinated at 900°C, 800°C, 700°C, and purchased calcium oxide.

Table 1. The surface area total of calcium oxide comparison of four approaches

Resources	BET Surface Area (m^2/g)
Calcined at 900°C	244.5211
Calcined at 800°C	232.7527
Calcined at 700°C	205.3055
Purchased	122.9513

The increase in specific surface area with increasing calcination temperature can be attributed to the decomposition of $CaCO_3$, which releases CO_2 and contributes to the formation of porous structures within the material. This process enhances pore development in CaO. However, at higher temperatures, sintering of CaO particles may also occur, which can potentially reduce surface area due to partial pore collapse or particle agglomeration. Therefore, the observed trend is considered to result from a balance between pore formation due to thermal decomposition and possible densification effects at elevated temperatures.

The crystalline structure and phase composition of the calcium oxide (CaO) products were analyzed using powder X-ray diffraction (PXRD). The diffraction patterns of purchased CaO and samples derived from golden snail shells calcined at different temperatures are presented in **Fig. 3**.

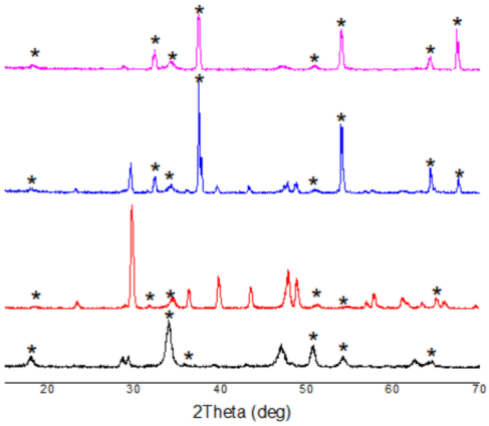

Figure 3 PXRD patterns of (a) calcium oxide calcinated at 900ºC, (b) 800ºC, (c) 700ºC, and (d) purchased calcium oxide.

The diffraction peaks correspond well with the standard CaO phase reported in previous literature, suggesting the formation of CaO from the calcined golden snail shell samples, particularly at higher calcination temperatures. The characteristic CaO peaks are observed at approximately 2θ = 32°; 37.2°; 53.7°[16]; 2θ at 18.02°, 34.12° and 50.85° [18]; 2θ at 53.9°, 64.2°, and 67.4° [20], which are consistent with reported CaO crystalline structures.

In addition to CaO, diffraction peaks observed at around 18.0° and 34.1° may be attributed to $Ca(OH)_2$ formation, which likely results from hydration of CaO upon exposure to atmospheric moisture after calcination. Furthermore, weak reflections associated with $CaCO_3$ may still be present, particularly in samples calcined at 700°C and 800°C, indicating incomplete thermal decomposition at lower temperatures.

The intensity of CaO peaks increases with increasing calcination temperature, indicating improved crystallinity and phase purity. Meanwhile, the reduction of $CaCO_3$ and $Ca(OH)_2$ related peaks suggests progressive decomposition and transformation toward CaO formation. Overall, the diffraction peaks correspond well with the standard CaO phase reported in previous literature, suggesting successful formation of CaO from the calcined golden snail shell samples, particularly at higher calcination temperatures.

4 Conclusion

Calcium oxide-rich materials were produced from golden snail shells through calcination at 700, 800, and 900°C for 5 hours. XRD analysis indicated the formation of crystalline CaO, while FTIR spectra suggested the presence of Ca-O bonds as well as possible carbonate and hydroxyl species due to residual $CaCO_3$ or surface carbonation/hydration. BET analysis showed that the sample calcined at 900°C exhibited the highest surface area among the prepared samples. However, further quantitative phase analysis and compositional characterization are required to confirm the purity of CaO and to evaluate the influence of residual impurities from the shell precursor.

The obtained CaO demonstrated favorable structural characteristics and surface properties, indicating its potential utilization in adsorption and catalytic applications. The use of golden snail shell waste from Tana Toraja also contributes to local biomass waste valorization and supports environmentally sustainable material processing.

.

Acknowledgement

The authors are grateful to the grant from State Polytechnic of Ujung Pandang (No.0043/PL10.11/AL.04/2023, 10 May 2023).

References

[1] Maftukhah S, Agustine D, Heri SM, Arrizal H, 2022, Application of golden snail shell powder as a river water purifier. In *ICSST 2021: Proceedings of the 1st International Conference on Social, Science, and Technology, ICSST 2021, 25 November 2021, Tangerang, Indonesia* (p. 304). European Alliance for Innovation. http://dx.doi.org/10.4108/eai.25-11-2021.2318850

[2] Hadi NH, Muhaimin MH, Redjeki S, 2024, Preparation of Calcinite Fertilizer from Golden Snail Shells by Calcination and Crystallization Processes, *Advance Sustainable Science Engineering and Technology*, *6*(4), 0240403-0240403. https://doi.org/10.26877/asset.v6i4.788

[3] Hwidi RS, Izhar TNT, Saad FNM, Dahham OS, Noriman NZ, Shayfull Z, 2018, Characterization of quicklime as raw material to hydrated lime: Effect of temperature on its characteristics, In *AIP conference proceedings* (Vol. 2030, No. 1, p. 020027). AIP Publishing LLC. https://doi.org/10.1063/1.5066668

[4] Rodiah S, Aprilia R, Ariesta N, 2022, Utilization Waste Materials to Synthesize Nano Al_2O_3-CaO Photocatalyst using Infused Red Guava Leaves (*Psidium Guajava* L.), *Al-Kimia*, *10*(2):180-191. https://doi.org/10.24252/al-kimia.v10i2.33481

[5] Jefri SR, Rodiah S, 2022, CaO Adsorbent

For Reducing Metal Content of Fe, Mn, and Zn from Pet-Set Waste-Water, *Jambura Journal of Health Sciences and Research*, *4*(3): 969-975. https://doi.org/10.35971/jjhsr.v4i3.16094

[6] Karim KR, Firnanelty F, Fadhilah N, 2025, Adsorption of Inorganic and Organic Waste of Chemistry Laboratory by Using Eggshell-Based CaO, *Indo. J. Chem. Res.,* 13(2): 168-175. https://doi.org/10.30598//ijcr.2025.13-kur

[7] Goksu A, Ruiz SC, Reina TR, Duyar M, 2025, Unveiling the potential of CaO-modified ZnO adsorbents for CO_2 capture. *Carbon Capture Science & Technology*, 100484. https://doi.org/10.1016/j.ccst.2025.100484

[8] Buasri A, Kamsuwan J, Dokput J, Buakaeo P, Horthong P, Loryuenyong V, 2024, Green synthesis of metal oxides (CaO-K_2O) catalyst using golden apple snail shell and cultivated banana peel for production of biofuel from non-edible Jatropha Curcas oil (JCO) via a central composite design (CCD), *Journal of Saudi Chemical Society*, 28(3): 101836. https://doi.org/10.1016/j.jscs.2024.101836

[9] Narasimharao K, Mostafa MMM, Al-Amshany ZM, Bajafar W, 2023, Mechanochemical synthesized $CaO/ZnCo_2O_4$ nanocomposites for biodiesel production, *Catalysts*, 13(2): 398. https://doi.org/10.3390/catal13020398

[10] de Sousa FP, dos Reis GP, Cardoso CC, Mussel WN, Pasa VM, 2016, Performance of CaO from different sources as a catalyst precursor in soybean oil transesterification: Kinetics and leaching evaluation, *Journal of environmental chemical engineering*, 4(2), 1970-1977. https://doi.org/10.1016/j.jece.2016.03.009

[11] Rahman F, Rodiah S, 2020, The Effect of CaO Catalyst Mass from Golden Snail Shell (*Pomacea Canaliculata* Lamarck) on Transesterification Reaction, *ALKIMIA: Jurnal Ilmu Kimia dan Terapan*, 4(2): 88-92. https://doi.org/10.19109/alkimia.v4i2.8084

[12] Mohamed F, Shaban M, Aljohani G, Ahmed AM, 2021, Synthesis of novel eco-friendly CaO/C photocatalyst from coffee and eggshell wastes for dye degradation, *Journal of Materials Research and Technology*, 14, 3140-3149. https://doi.org/10.1016/j.jmrt.2021.08.055

[13] Correia LM, Saboya RMA, de Sousa Campelo N, Cecilia JA, Rodríguez-Castellón E, Cavalcante Jr CL, Vieira RS, 2014, Characterization of calcium oxide catalysts from natural sources and their application in the transesterification of sunflower oil, *Bioresource technology*, *151*, 207-213. https://doi.org/10.1016/j.biortech.2013.10.046

[14] Kumar S, Sharma V, Pradhan JK, Sharma S K, Singh P, Sharma JK, 2021, Structural, Optical and Antibacterial Response of CaO Nanoparticles Synthesized via Direct Precipitation Technique, *Nano Biomedicine & Engineering*, 13(2). https://doi.org/10.5101/NBE.V13I2.P172-178

[15] Khine EE, Koncz-Horvath D, Kristaly F, Ferenczi T, Karacs G, Baumli P, Kaptay G, 2022, Synthesis and characterization of calcium oxide nanoparticles for CO_2 capture, *Journal of Nanoparticle Research*, 24(7), 139. https://doi.org/10.1007/s11051-022-05518-z

[16] Huh JH, Choi YH, Ramakrishna C, Cheong SH, Ahn JW, 2016, Use of calcined oyster shell powders as CO_2 adsorbents in algae-containing water, *Journal of the Korean Ceramic Society*, 53(4): 429-434. https://doi.org/10.4191/kcers.2016.53.4.429

[17] Naeem MA, Armutlulu A, Imtiaz Q, Donat F, Schäublin R, Kierzkowska A, Müller CR, 2018, Optimization of the structural characteristics of CaO and its effective stabilization yield high-capacity CO_2 sorbents, *Nature communications*, 9(1): 2408. https://doi.org/10.1038/s41467-018-04794-5

[18] Ramli M, Rossani RB, Nadia Y, Darmawan TB, Febriani, Saiful, Ismail YS, 2019, Nanoparticle fabrication of calcium oxide (CaO) mediated by the extract of red dragon fruit peels (*Hylocereus Polyrhizus*) and its application as inorganic–anti-microorganism materials, In *IOP conference series: materials science and engineering* (Vol. 509, No. 1, p. 012090), IOP Publishing. https://doi.org/10.1088/1757-899X/509/1/012090

[19] Hussein AI, Ab-Ghani Z, Che Mat AN, Ab Ghani NA, Husein A, Ab Rahman I, 2020, Synthesis and characterization of spherical calcium carbonate nanoparticles derived from cockle shells, *Applied Sciences*, 10(20): 7170. https://doi.org/10.3390/app10207170

[20] Zhu Y, Wu S, Wang X, 2011, Nano CaO grain characteristics and growth model under calcination, *Chemical Engineering Journal*, 175: 512-518.

https://doi.org/10.1016/j.cej.2011.09.084

[21] Damayanti JD, Ole MAN, Rustan R, Ananda AD, Riyadi NA, 2024, Calcination temperature effects on CaO yield from golden snail shells (*Pomacea canaliculata* L.) waste, In *AIP Conference Proceedings* (Vol. 3140, No. 1, p. 060005). AIP Publishing LLC. https://doi.org/10.1063/5.0221161